




Comment on “Tuning topological surface states by cleavage angle in topological crystalline insulators”

R. Buczko * and P. Kacman 

Institute of Physics, Polish Academy of Sciences, Al. Lotników 32/46, 02-668 Warsaw, Poland

 (Received 29 November 2019; revised manuscript received 5 February 2020; accepted 24 March 2020; published 20 April 2020)

The results of the commented paper seem to disagree with the prediction of the paper by Safaei *et al.* [*Phys. Rev. B* **88**, 045305 (2013)]. Some of the definitions of surface unit cells used in the commented article do not lead to the first surface Brillouin zone, defining instead a folded Brillouin zone. This is the source of the seeming discrepancies. To dispel the misunderstandings we present general rules for Brillouin zone shapes and L points projections for $\{ppq\}$ surfaces of the rock salt crystals. We show that using the first Brillouin zones allows a simple, straightforward prediction of the topological properties of the surface states.

DOI: [10.1103/PhysRevB.101.157103](https://doi.org/10.1103/PhysRevB.101.157103)

I. COMMENT

Plekhanov and Weber in their paper [1] discuss the interesting topic of topologically protected surface states in the recently widely studied class of materials, i.e., topological crystalline insulators (TCI). The authors study the existence of such states on surfaces of IV-VI TCI inclined at small angles to the three main surfaces: (001), (110), and (111), which were discussed already in detail in Refs. [2] and [3]. It should be noted here that in Ref. [2] the existence of topologically protected surface states for other surfaces was also predicted. Namely, in Ref. [2] (in the Discussion section and in the Appendix) it was pointed out that surface states with at least two protected Dirac points appear on all $\{ppq\}$ -type surfaces.

In IV-VI TCI the energy gaps in L points of the bulk Brillouin zone (BZ) are inverted. Thus, one can expect that in the surface 2D BZ Dirac points should appear at the L point projections. They are topologically protected (TP), however, only for $\{ppq\}$ -type surfaces, which are symmetric about any of the $\{110\}$ mirror planes. The TP projection points should be situated at the mirror line. On the other hand we note that all four nonequivalent L points as well as their projections are time reversal symmetric (TRS). We also note that the eigenstates of the mirror plane symmetry operators form $\pm\vec{k}$ Kramers pairs. When the L points are projected separately, single Dirac points should appear exactly in TP TRS points, where these pairs are degenerate. When two L points are projected to the same point of 2D BZ, then two TRS Dirac points will be energetically split by valley interaction and two secondary crossings (also called Dirac points) should appear along the mirror line. In this case the Kramers pairs are formed by opposite mirror plane symmetry eigenstates in the two $\pm\vec{k}$ split secondary crossings. In Refs. [2–4] two special cases, i.e. $\{001\}$ and $\{111\}$ surfaces were considered. Indeed, it was shown that for $\{111\}$ surfaces the L points are

projected separately to four TP TRS points, whereas in the $\{001\}$ surfaces they are projected in two pairs to two such points. For other $\{ppq\}$ surfaces, depending on the parities of p and q numbers, either two single or one double projection to the TP TRS points take place. In our work [2], we have shown that when the parities of p and q are the same the L points are projected in pairs, while for opposite parities the L points are projected separately. This result holds for p and q which are relatively prime. Of course other surface definitions can be reduced to those with relatively prime indices. Thus, the same parity of p and q means that they are odd numbers. In the following text we will assume that p and q indices are always co-prime. As shown in the next section, 2D BZ of a surface with indices of opposite parity has a rectangular shape. The L points are projected in pairs to the topologically protected \bar{X} point and unprotected \bar{M} or \bar{Y} point (we use here the same notation for the high symmetry points of BZ as given in Ref. [1], which is different from that in Ref. [2]). Finally, we note that for indices of the same (odd) parity the shape of BZ is hexagonal and the points are projected separately: one to $\bar{\Gamma}$ (protected), another one to the protected \bar{M} point, and two to the other two unprotected \bar{M} points. In this case \bar{M} points are situated in the middle of the hexagon edges. Examples of such 2D BZs are presented in Figs. 1(a) and 1(b).

The results of Ref. [1] seemingly differ from the above predictions. This is probably the reason that the authors, when citing our paper, claim that we take into account only the three main surfaces. A careful analysis shows, however, that our predictions are in reality confirmed in Ref. [1]. The source of the seeming discrepancy lies in the definition of the surfaces and their unit cells in Ref. [1]. The authors define the inclined surfaces by fixing two vectors b_1 and b_2 of the surface unit cell and the vector b_3 perpendicular to the surface. These vectors determine the surface indices. The definitions in the paper do not always lead to the primitive unit cells. Although we agree that one can define the unit cells in different ways and we understand that the choice made in Ref. [1] was convenient for performing the calculations, in our opinion it is not apposite

*buczko@ifpan.edu.pl

for the discussion of results. For example, for surfaces tilted in respect to (001) and (110) the indices are: $(m, m, -2n)$. As can be seen the n and m parameters given in Table I determine surfaces with coprime indices of opposite parities, p odd and q even. It means that in all presented cases the pair of Dirac points in the \bar{X} point should be TP and the other pair should be in the topologically nonprotected (TNP) \bar{M} point. In Table I such classification appears only for half of the cases. For the other half $\bar{\Gamma}$ as the TP point and \bar{Y} as TNP are reported. In the latter, the surface unit cells defined by the authors are twice longer in the direction perpendicular to $[1, -1, 0]$ than the primitive cell. Accordingly, they lead to a folded BZ. Thus, the points \bar{X} and \bar{M} of BZ are folded into $\bar{\Gamma}$ and \bar{Y} .

Next, Table III presents results for surfaces tilted to (110) with surface indices given by $(m; m; -2n)$. Also here, when different than primitive unit cells are used, the classification of TP points is different than expected. In particular, for the surface defined by $n = 4$ and $m = 10$ (i.e., $p = 5$ and $q = 4$), the TP point in the unfolded BZ should be X and the TNP point should appear in M . In the other two cases: $n = 1, m = 10$ and $n = 1, m = 6$, the relatively prime surface indices p and q are odd. It means that the unfolded BZ should be hexagonal with two TP points: one in $\bar{\Gamma}$ and the other in \bar{M} . The two TNP points should be now in the two remaining \bar{M} points [see the illustration in Fig. 1(b)]. In the case of surfaces tilted to (111) (Table II), the authors do not recognize that for $n = 1$ the surface is (001), thus both \bar{X} and \bar{Y} points are TP. The energy spectrum presented in Fig. 3 of the paper also corresponds to the (001) surface. Furthermore, it should be noted that Figs. 4(a) and 2(b) present equivalent surfaces belonging to the same $\{114\}$ family. The illustration in Fig. 2(b) differs from that in Fig. 4(a), because in the former (as in several other figures) the BZ is folded and, therefore, two times smaller than the first BZ.

Finally, the authors wrote “in the limit $\theta = 0$ each surface TRS point acquires the projections from two L points, which then form a bonding and anti-bonding combinations.” One can easily check that all four nonequivalent L points of the 3D BZ are projected in two pairs, one pair to \bar{X} and the other either to \bar{Y} or \bar{M} not only for n approaching an infinite value but for all surfaces with indices p and q of opposite parity. As shown in all discussed above cases, using the primitive unit cells and unfolded BZs is essential for a unique classification of TP and TNP points. It allows us also to distinguish between TP single and double Dirac points. Using folded BZ is not a mistake, but it does not allow to get such useful results.

II. BRILLOUIN ZONE SHAPES AND L POINTS PROJECTIONS FOR (ppq) SURFACES OF CUBIC FACE-CENTERED CRYSTALS. GENERAL RULES.

To clarify the description of the existence of topological states on inclined surfaces we present general rules for the construction of Brillouin zones for any (ppq) surface in a cubic face-centered structure, in particular in a rock salt crystal. We present conditions leading to either rectangular or hexagonal shapes of the 2D BZ as well as show how L points projections depend on the parity of p and q numbers.

A. Primitive surface lattice vectors

In the cubic face-centered crystals atoms of the same type form rows in $\langle 110 \rangle$ directions. The distance between neighboring atoms in the row is equal to $a/\sqrt{2}$, where a is the lattice constant in the bulk. Because the $[1\bar{1}0]$ direction is parallel to any (ppq) plane, every (ppq) surface is formed by atomic rows at various altitudes. Here and hereafter we discuss only surfaces which can be obtained as cuts of the bulk crystal without reconstruction of atomic positions.

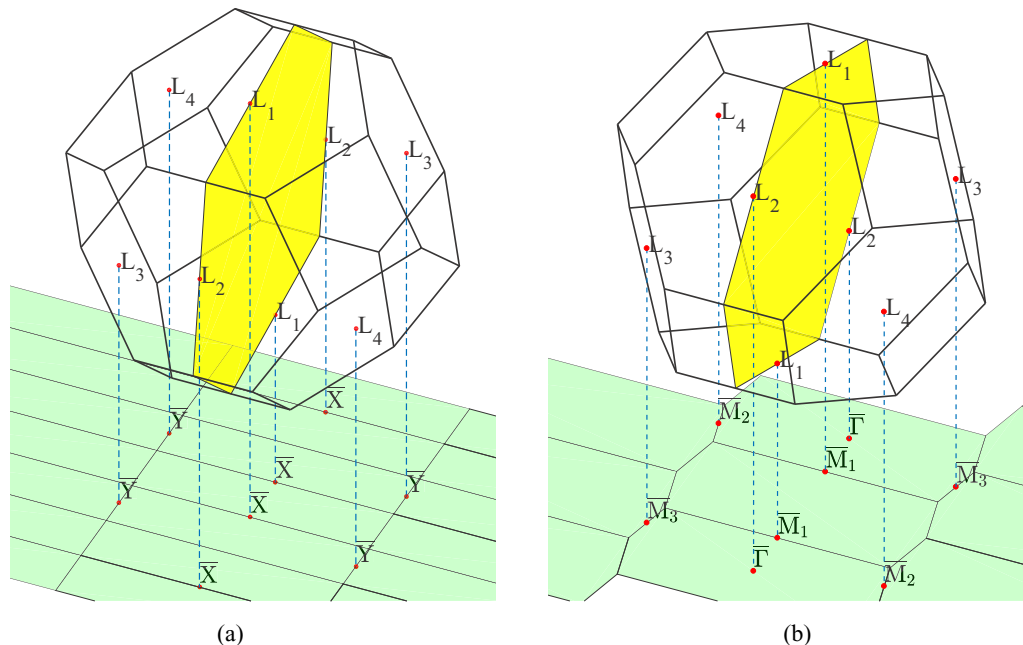


FIG. 1. Three-dimensional view of the multiple (a) rectangular (223) and (b) hexagonal (331) surface 2D BZs with L -points projections. The $(1\bar{1}0)$ mirror plane inside the bulk BZ is marked in yellow.

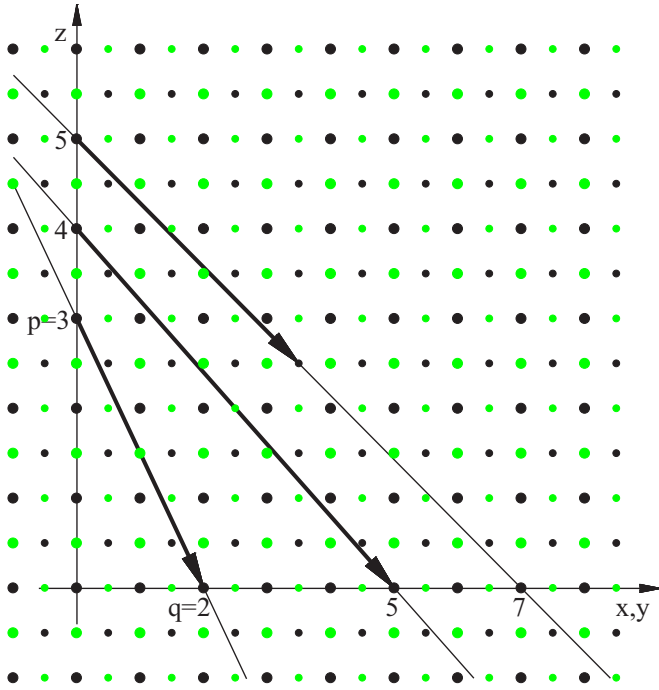


FIG. 2. View of the $(1\bar{1}0)$ rock salt crystal cross section. The projections of three planes, (332), (445), and (557), into this cross section are shown as three oblique lines.

In Fig. 2 the $(1\bar{1}0)$ rock salt crystal cross section is presented. In the figure each row of atoms perpendicular to this cross section is represented by one dot (black for cations and green for anions). Dots with the same radius correspond to rows of atoms having the same coordinates along the $[1\bar{1}0]$ axis. The bigger dots represent rows with an atom lying on the cross section, while rows of atoms with positions shifted by $a/(2\sqrt{2})$ are depicted by smaller dots. Atoms in the rows are positioned periodically with the primitive lattice vector given by:

$$\vec{t}_1 = \frac{a}{2} \begin{pmatrix} 1 \\ -1 \\ 0 \end{pmatrix}. \quad (1)$$

In order to find the second primitive vector \vec{t}_2 let us first discuss the lattice vector \vec{t}_\perp in the (ppq) plane in the direction perpendicular to \vec{t}_1 . We choose the origin of the coordinate system at one of the cations shown in Fig. 2. The z axis points in the $[001]$ direction. Axes x and y (in $[100]$ and $[010]$ directions) are shown in the figure as the projections on the $(1\bar{1}0)$ cross section. Let us consider various (ppq) planes which cross the x , y and z axes at q , q and p coordinates. In Fig. 2 the projections of three such planes, (332), (445) and (557), into the crystal cross section are shown as three oblique lines. For each of these planes the vector \vec{t}_\perp should point along this line and connect pairs of atoms represented by dots of the same color and radius. Thus,

$$\vec{t}_\perp = \frac{a}{2} \begin{pmatrix} q \\ q \\ -2p \end{pmatrix}. \quad (2)$$

One can find that:

$$\vec{t}_\perp = -p(\vec{t}_1 + \vec{t}_2) + (p+q)\vec{t}_3, \quad \text{where} \quad (3)$$

$$\vec{t}_1 = \frac{a}{2} \begin{pmatrix} 0 \\ 1 \\ 1 \end{pmatrix}, \quad \vec{t}_2 = \frac{a}{2} \begin{pmatrix} 1 \\ 0 \\ 1 \end{pmatrix}, \quad \vec{t}_3 = \frac{a}{2} \begin{pmatrix} 1 \\ 1 \\ 0 \end{pmatrix} \quad (4)$$

are primitive vectors of the bulk lattice. Because the pair of integer numbers p and q is relatively prime also the pair p and $p+q$ is co-prime. Thus, there is no shorter lattice vector t_\perp than that given by Eq. (2).

When p and q have opposite parities there are no lattice vectors shorter than \vec{t}_1 and \vec{t}_\perp and thus the second primitive vector is $\vec{t}_2 = \vec{t}_\perp$. When p and q are both odd numbers, then and only then one can find that both types of atomic rows (shifted and not shifted) belong to the same (ppq) plane. In this case a surface lattice vector \vec{t}_2 shorter than t_\perp and not perpendicular to t_1 can be found. This \vec{t}_2 is the shortest lattice vector connecting atoms in shifted and not shifted rows.

$$\begin{aligned} \vec{t}_2 &= \frac{1}{2}(\vec{t}_\perp + \vec{t}_1) = \frac{a}{4} \begin{pmatrix} q+1 \\ q-1 \\ -2p \end{pmatrix} = -\frac{1}{2}(p+1)\vec{t}_1 \\ &\quad - \frac{1}{2}(p-1)\vec{t}_2 + \frac{1}{2}(p+q)\vec{t}_3 \end{aligned} \quad (5)$$

The integers $(p+1)/2$, $(p-1)/2$, and $(p+q)/2$ are relatively prime for odd p and q .

Vectors \vec{t}_2 for three different surfaces are shown in Fig. 2. We note that in the case of (557) \vec{t}_2 is not in the cross section plane and what is shown in the figure is its projection. For p and q both odd another interesting observation can be made, again not noticed in Ref. [1]. Namely, in the case of rock salt structure two types of surfaces exist: In the first type the highest row contains cations while in the second type anions.

B. Reciprocal lattice vectors

With the use of \vec{t}_1 and \vec{t}_2 one can find reciprocal lattice vectors \vec{G}_1 and \vec{G}_2 .

For p and q with different parities:

$$\vec{G}_1 = \frac{2\pi}{a} \begin{pmatrix} 1 \\ -1 \\ 0 \end{pmatrix}, \quad \vec{G}_2 = \frac{2\pi}{a(2p^2 + q^2)} \begin{pmatrix} q \\ q \\ -2p \end{pmatrix}. \quad (6)$$

The vector \vec{G}_1 is perpendicular to \vec{G}_2 due to the orthogonality of \vec{t}_1 and \vec{t}_2 . In this case BZ has a rectangular shape. In contrast, when p and q are both odd, the vectors \vec{G} :

$$\begin{aligned} \vec{G}_1 &= \frac{2\pi}{a} \begin{pmatrix} 1 \\ -1 \\ 0 \end{pmatrix} - \frac{2\pi}{a(2p^2 + q^2)} \begin{pmatrix} q \\ q \\ -2p \end{pmatrix}, \\ \vec{G}_2 &= \frac{4\pi}{a(2p^2 + q^2)} \begin{pmatrix} q \\ q \\ -2p \end{pmatrix} \end{aligned} \quad (7)$$

are not orthogonal and BZ is hexagonal.

TABLE I. The dependence of the shape of the 2D BZ, type of the L point projections, and their topological protection on the parity of p and q numbers. The two special cases, i.e., (001) and (111) surfaces, are shown in the two first rows.

p	q	BZ	projection	TP	TNP
0	1	rectangular	double	\bar{X}_1, \bar{X}_2	
1	1	hexagonal	single	$\bar{\Gamma}, \bar{M}_1, \bar{M}_2, \bar{M}_3$	
odd	odd	hexagonal	single	$\bar{\Gamma}, \bar{M}_1$	\bar{M}_2, \bar{M}_3
odd	even	rectangular	double	\bar{X}	\bar{M}
even	odd	rectangular	double	\bar{X}	\bar{Y}

C. L points projections

As already mentioned, in our paper [2] we have shown that all four nonequivalent L points in the Brillouin zone of the bulk crystal project to high symmetry points of the surface 2D BZ either separately or in pairs, depending on the parity of p and q numbers. As the L points are TRS points, their projections should be TRS points in the 2D reciprocal space. We note also that in a 2D BZ there are always only four TRS points.

Let us first consider p and q both odd, in which case the L points project separately to four points of the hexagonal 2D BZ. Here the four TRS points are: $\bar{\Gamma}$ in the middle

of 2D BZ and three \bar{M} points in the middle of BZ edges ($\bar{M}_1 = \frac{1}{2}\bar{G}_2$, $\bar{M}_2 = \frac{1}{2}\bar{G}_1$, $\bar{M}_3 = \frac{1}{2}(\bar{G}_1 + \bar{G}_2)$). All of them are L point projections.

The case of p and q with opposite parities is more complicated. We know already that in this case the L points are projected in pairs to two TRS points in 2D BZ of rectangular shape. Using similar methods as presented in the Appendix to the paper [2] and using properties of the relatively prime numbers we can show that:

(1) when p is even and q odd, L points are projected in two pairs to $\bar{X} = \frac{1}{2}\bar{G}_2$ and $\bar{Y} = \frac{1}{2}\bar{G}_1$;

(2) when p is odd and q even, L points are projected in two pairs to \bar{X} and $\bar{M} = \frac{1}{2}(\bar{G}_1 + \bar{G}_2)$ points.

In summary, in this comment we have shown that for any $\{ppq\}$ -type surface the shape of the 2D BZ as well as the way in which the L points are projected to the TRS points (both, topologically protected TP and not protected TNP points) depend on the parity of the p and q numbers, as shown in Table I.

ACKNOWLEDGMENT

This work was supported by the Polish National Science Center under project 2016/23/B/ST3/03725.

[1] E. Plekhanov and C. Weber, *Phys. Rev. B* **100**, 115161 (2019).
 [2] S. Safaei, P. Kacman, and R. Buczko, *Phys. Rev. B* **88**, 045305 (2013).

[3] J. Liu, W. Duan, and L. Fu, *Phys. Rev. B* **88**, 241303 (2013).
 [4] T. H. Hsieh, H. Lin, J. Liu, W. Duan, A. Bansil, and L. Fu, *Nat. Commun.* **3**, 982 (2012).